Assignment of ^{1}H, ^{15}N, and ^{13}C Resonances, Identification of Elements of Secondary Structure and Determination of the Global Fold of the DNA-Binding Domain of GAL4†

Masahiro Shirakawa,‡ Wayne J. Fairbrother,§,∥ Yasuharu Serikawa,‡ Tadayasu Ohkubo,⊥ Yoshimasa Kyogoku,*,‡ and Peter E. Wright*,§

Institute for Protein Research, Osaka University, Suita, Osaka 565, Japan, Department of Molecular Biology, The Scripps Research Institute, La Jolla, California 92037, and Protein Engineering Research Institute, Suita, Osaka 565, Japan

Received October 20, 1992

ABSTRACT: Almost complete assignments of the ^{1}H, ^{15}N, and aliphatic ^{13}C resonances of the 62-residue N-terminal DNA-binding domain of GAL4 [GAL4(62)] have been obtained using a combination of two-dimensional homonuclear and two- and three-dimensional double- and triple-resonance heteronuclear NMR methods. The sequential NOE connectivities, amide proton exchange measurements, and $^{13}C\alpha$ chemical shift data indicate the presence of two short α-helices in the N-terminal half of the polypeptide. Residues 1–9 and 41–62 appear to be unstructured and flexible in solution. Analysis of the $^{13}C\alpha$ chemical shifts also revealed a significant downfield shift of approximately +3 ppm, relative to random-coil values, for the four nonbridging Zn(II) ligands, Cys 14, 21, 31, and 38. Interestingly, no such correlation was observed for the two bridging ligands, Cys 11 and 28. Preliminary structure calculations using a subset of distance restraints derived from three-dimensional ^{1}H–^{15}N and ^{1}H–^{13}C NOESY-HSQC spectra are consistent with the recently reported solution structures of $Zn(II)_2$GAL4(7–49) [Kraulis, P., et al. (1992) *Nature 356,* 448–450] and of $Cd(II)_2$GAL4(65) [Baleja, J. D., et al. (1992) *Nature 356,* 450–453].

GAL4, a transcriptional activator protein from *Saccharomyces cerevisiae*, binds specifically to a 17 base-pair palindromic DNA sequence known as UAS_G (Giniger et al., 1985) and is responsible for induction of the genes required for galactose catabolism (Oshima, 1981). The specific DNA-binding domain of the 881-residue GAL4 protein has been defined as the N-terminal 74 amino acids by deletion mutagenesis (Ma & Ptashne, 1987). We have previously shown that a GAL4 fragment comprising the 96 N-terminal amino acids, expressed in *Escherichia coli*, has specific binding activity to UAS_G and that Zn(II) is required for maintenance of the protein conformation as well as for the specific DNA binding (Serikawa et al., 1990). Pan and Coleman (1990a) have reported that an N-terminal GAL4 fragment consisting of the first 62 residues, expressed in *E. coli*, bound to DNA when it was chemically dimerized.

The N-terminal DNA-binding domain of GAL4 contains a sequence of six cysteine residues (Laughon & Gesteland, 1984), forming a Cys-X_2-Cys-X_6-Cys-X_6-Cys-X_2-Cys-X_6-Cys motif which is conserved among 11 fungal transcription factors (Andre, 1990). At first it was thought that the domain contained a cysteine–zinc finger comprising a zinc ion bound between two pairs of cysteine residues (Rhodes & Klug, 1988). However, contrary to these expectations, two Cd(II) or two Zn(II) ions were shown to bind tightly to the DNA-binding domain of GAL4, and a $Zn(II)_2Cys_6$ binuclear cluster was proposed for the native protein (Pan & Coleman, 1990b, 1991; Gadhavi et al., 1991).

We report here extensive ^{1}H, ^{15}N, and ^{13}C assignments of the 62-residue N-terminal fragment of GAL4 [GAL4(62)] obtained from two- and three-dimensional heteronuclear NMR experiments, the elucidation of the secondary structure, and preliminary structure calculations, based on short-, medium-, and long-range NOEs, which establish the global fold of the protein. The assignment strategy used is similar to that reported previously for several larger proteins, with the backbone ^{1}H and ^{15}N resonances first being assigned using principally three-dimensional (3D) ^{15}N-edited TOCSY and NOESY experiments (Driscoll et al., 1990; Carr et al., 1991; Fairbrother et al., 1991; Clubb et al., 1991; Redfield et al., 1991; Stockman et al., 1992; Wang et al., 1992; van Nuland et al., 1992; Borden et al., 1992), followed by assignment of the aliphatic ^{1}H and ^{13}C resonances using a combination of 3D triple-resonance and HCCH experiments (Clore et al., 1990; Fairbrother et al., 1992). The pattern of sequential NOEs observed in the 3D ^{1}H–^{15}N NOESY-HSQC spectrum, analysis of the $^{13}C\alpha$ chemical shifts, and preliminary structure calculations, performed using distance constraints derived from 3D ^{1}H–^{15}N NOESY-HSQC and ^{1}H–^{13}C NOESY-HSQC spectra, indicate that the presence of two α-helices in GAL4-(62). The preliminary solution structure obtained here for GAL4(62) is similar to those recently reported for GAL4-(65) (Baleja et al., 1992) and for the smaller fragment GAL4-(7–49) (Kraulis et al., 1992).

MATERIALS AND METHODS

Sample Preparation. A *Bam*HI–*Hin*fI DNA fragment from plasmid pGT96 (Serikawa et al., 1990), which codes for residues 1–58 of the GAL4 protein, was cloned into a *Bam*HI–

† This work was supported by a Grant-in-Aid for Special Project Research from the Ministry of Education, Science and Culture of Japan (No. 03259103), by Special Coordination Funds from the Science Technology Agency, by a Japan–U.S. Cooperative Science Program Grant administered jointly by the Japan Society for the Promotion of Science and the U.S. National Science Foundation, and by the National Institutes of Health (GM 36643). M.S. was partly supported by Toyobo Biotechnology Foundation. W.J.F. was supported by a Damon Runyon-Walter Winchell Cancer Research Fund Fellowship (DRG-1059).

* To whom correspondence should be addressed.

‡ Osaka University.

§ The Scripps Research Institute.

∥ Present address: Genentech, Inc., Department of Protein Engineering, 460 Point San Bruno Blvd., South San Francisco, CA 94080.

⊥ Protein Engineering Research Institute, Osaka.

0006-2960/93/0432-2144$04.00/0

*Sal*I site within the polylinker site of pKP1500 (Miki et al., 1987) with the aid of a double-stranded oligonucleotide [d(AATCTAGACTCGAGTAAG)/d(TGGACTTACTCGAGTCTAG)] as an adapter DNA which codes amino acids 59–62 of GAL4 and possesses a stop codon and *Sal*I end. The oligonucleotides were synthesized with an automated synthesizer (Applied Biosystems 380B). The resulting plasmid, pGT62, contains the gene for GAL4(62) under the control of the strong inducible *tac* promoter.

All the GAL4(62) samples were derived from transformed *E. coli* (strain TG1) cells containing the expression plasmid pGT62. The harvested cell paste was resuspended in a lysis buffer (10 mM Tris-HCl, pH 7.8, 300 mM KCl, 1 mM phenylmethane sulfonyl fluoride, 7 mM 2-mercaptoethanol) followed by sonication for 20 min on ice. The insoluble materials were removed by centrifugation at 20000*g* for 15 min at 4 °C. The soluble fraction was loaded directly onto a DE-52 column (Pharmacia). The eluate was concentrated by precipitation with 75% saturated ammonium sulfate, followed by dialysis against a buffer containing 50 mM phosphate, 50 mM KCl, and 7 mM 2-mercaptoethanol at pH 6.8. The dialysate was then loaded onto a S-sepharose column (Pharmacia) preequilibrated with B-buffer (50 mM phosphate, pH 6.8, 7 mM 2-mercaptoethanol) containing 50 mM KCl. The protein was eluted with a KCl gradient formed from B-buffer plus 50–1000 mM KCl. GAL4(62) eluted in the 400–600 mM KCl fractions and was then dialyzed against B-buffer containing 50 mM KCl. The dialysate was then loaded onto a mono-S column (Pharmacia) and eluted with a KCl gradient formed from B-buffer plus 50–500 mM KCl. The protein was eluted in the 400 mM KCl fractions and was purified to >95%. We obtained >2 mg of GAL4(62) from 1 L of bacterial culture. Uniformly ^{15}N- or $^{15}N/^{13}C$-labeled GAL4(62) was obtained from bacteria grown in M9 medium with $^{15}NH_4Cl$ and [$^{13}C_6$]D-glucose as the sole nitrogen and carbon sources, respectively.

The samples for NMR measurements typically comprised 1–2 mM protein in 90% H_2O/10% D_2O, or in D_2O, containing 5 mM phosphate buffer and 50 mM KCl at pH 5.5 (direct meter reading).

NMR Spectroscopy. All two-dimensional (2D) ^1H–^1H spectra were acquired on a Bruker AM-600 spectrometer. Homonuclear 2D DQF-COSY, TOCSY, and NOESY spectra were recorded at 30 and 40 °C, typically using spectral widths of 8333 Hz in both dimensions, with 512 t_1 increments of 4K complex data points. The 2D ^1H–^{15}N HSQC, ^1H–^{15}N HSQC-NOESY, and ^1H–^{15}N HSQC-TOCSY spectra (Bodenhausen & Ruben, 1980; Bax et al., 1990a; Norwood et al., 1990) of uniformly ^{15}N-labeled GAL4(62) were recorded on either a Bruker AM-600 or AM-500 spectrometer. Solvent suppression was achieved by presaturation during the relaxation delay or by the use of spin lock purge pulses (Messerle et al., 1989). ^{15}N decoupling during acquisition was achieved using GARP-1 phase modulation (Shaka et al., 1985). All 2D spectra were recorded in a pure absorption mode with t_1 quadrature detection achieved using time-proportional phase incrementation (TPPI; Redfield & Kunz, 1975; Marion & Wüthrich, 1983). Data were processed with an ASPECT 3000 computer or transferred to a Silicon Graphics Iris 4D/20GT workstation for processing and analysis using the FTNMR software package (Hare Research, Inc.).

The 3D ^1H–^{15}N TOCSY-HSQC and NOESY-HSQC spectra of uniformly ^{15}N-labeled GAL4(62) were recorded at 30 °C on a Bruker AM-600 spectrometer. The pulse sequences used were similar to those previously described for the TOCSY-HMQC and NOESY-HMQC experiments (Fairbrother et al., 1991) except for the addition of two ^1H 90°$_y$ pulses (one immediately preceding t_2 and the other immediately following t_2). This simple modification has the advantage of eliminating dispersive components in the NH/Hα cross peaks due to the $^3J_{NH\alpha}$ coupling. DIPSI-2 (Shaka et al., 1988; Rucker & Shaka, 1989) was used for ^1H isotropic mixing in the 3D ^1H–^{15}N TOCSY-HSQC experiment. The isotropic mixing time for the TOCSY-HSQC experiment was 81 ms, and the mixing time for the NOESY-HSQC experiment was 100 ms. The acquired data matrices of each 3D experiment were 128 (t_1) × 32 (t_2) × 1024 (t_3) complex points, and the spectral widths were 6793.5, 881.8, and 8928.6 Hz in F_1, F_2, and F_3, respectively. 3D data were processed on a Silicon Graphics Iris 4D/20GT workstation using FTNMR for the F_1–F_3 planes and a separate routine written by Dr. M. Rance (The Scripps Research Institute) for the F_2 Fourier transform. Each data matrix was zero-filled to 256 (F_1) × 64 (F_2) × 1024 (F_3) data points. The spectra were recorded in pure absorption mode using TPPI for quadrature detection in t_1 and TPPI-States (Marion et al., 1989a) for quadrature detection in t_2. Solvent suppression was achieved using spin lock purge pulses (Messerle et al., 1989) and by convolution of the time-domain data (Marion et al., 1989b).

Triple-resonance 3D HCA(CO)N and 3D HCCH-COSY and HCCH-TOCSY experiments were recorded at 30 °C using a Bruker AMX-500 spectrometer equipped with a three-channel interface. The pulses for the ^1H, aliphatic ^{13}C, carbonyl ^{13}C, and ^{15}N frequencies were generated using the proton, *X*-nucleus, and *Y*-nucleus channels of the spectrometer or a frequency synthesizer (PTS300, Programmed Test Sources) and a pulse amplifier (M3205, American Microwave Technology, Inc.). A home-built switch (Dr. M. Rance, The Scripps Research Institute) was used to gate the output of the synthesizer. A digital word generator (RS670, Interface Technology) was used to control the RF phase of the synthesizer in the triple-resonance HCA(CO)N experiment. Spectra were processed in a similar fashion to the 3D TOCSY-HSQC and NOESY-HSQC, discussed above.

The pulse sequence used for the 3D triple-resonance constant-time HCA(CO)N experiment was Scheme II of Palmer et al. (1992). The constant-time period, *T*, was set to 27 ms. GARP-1 phase modulation was used for aliphatic ^{13}C decoupling during acquisition. The ^1H carrier was placed at 4.7 ppm, the ^{15}N carrier at 122 ppm, and the $^{13}C\alpha$ carrier at 52.5 ppm. A total of 59 (t_1) × 32 (t_2) × 512 (t_3) complex data points were collected with spectral widths of 3333, 735, and 6250 Hz in F_1, F_2, and F_3, respectively. Zero-filling was employed to yield a final absorptive spectrum of 256 (F_1) × 64 (F_2) × 2048 (F_3) points. Suppression of the residual HDO resonance was achieved by low-power presaturation during the relaxation delay. Quadrature detection in t_1 and t_2 was achieved in the TPPI-States manner. Folding of the spectrum occurs in the F_2 dimension. The t_2 sampling delay was adjusted to be half of the increment, resulting in a −180° first-order phase correction being necessary in this dimension. As a result, the singly folded peaks have opposite phase to the unfolded and doubly folded peaks (Bax et al., 1991).

3D constant-time HCCH-COSY (Ikura et al., 1991a) and 3D HCCH-TOCSY (Bax et al., 1990b) spectra were acquired as previously described (Fairbrother et al., 1992). GARP-1 phase-modulation was used for ^{13}C decoupling during acquisition. The DIPSI-2 sequence was used for ^{13}C isotropic mixing in the 3D HCCH-TOCSY experiment. The ^1H carrier was placed at 3.0 ppm and the ^{13}C carrier at 41.3 ppm in both

experiments. The acquired data matrices were 128 (t_1) × 28 (t_2) × 512 (t_3) complex data points for the HCCH-COSY experiment and 128 (t_1) × 32 (t_2) × 512 (t_3) complex data points for the HCCH-TOCSY experiment. Spectral widths were 3937, 3937, and 12 500 Hz in the F_1, F_2, and F_3 dimensions, respectively, for the HCCH-COSY and 4000, 3937, and 12500 Hz in the F_1, F_2, and F_3 dimensions, respectively, for the HCCH-TOCSY experiment. The period $2T$ for the constant-time HCCH-COSY experiment was 7.8 ms, and the isotropic mixing time for the HCCH-TOCSY experiment was 23.1 ms. Both spectra were recorded in pure absorption mode using the TPPI-States method of quadrature detection in t_1 and the States method (States et al., 1982) in t_2. Suppression of the residual HDO resonance was achieved by low-power presaturation during the relaxation delay. Zero-filling was employed to yield a final absorptive spectrum of 512 (F_1) × 64 (F_2) × 1024 (F_3) points for both spectra. Folding occurs in the F_2 dimension of both HCCH experiments; spectra were therefore acquired such that the folded peaks had opposite phase to unfolded peaks (Bax et al., 1991).

The ^{1}H chemical shifts are given relative to external DSS, and the ^{15}N chemical shifts are given relative to external 3 M $HCO^{15}NH_2$. The ^{13}C chemical shifts were indirectly referenced to TMS by multiplying the spectrometer frequency corresponding to 0 ppm in the ^{1}H spectrum by the ^{13}C/^{1}H frequency ratio (0.25145002; Bax & Subramanian, 1986).

Structure Calculations. Distance constraints for preliminary structure calculations were derived mainly from a 100-ms mixing time 3D ^{1}H–^{15}N NOESY-HSQC spectrum obtained from a 2 mM sample of uniformly ^{15}N-labeled GAL4-(62) and a 100-ms mixing time 3D ^{1}H–^{13}C NOESY-HSQC spectrum of a 1.8 mM sample of uniformly ^{15}N/^{13}C-labeled GAL4(62). The NOEs were characterized on the basis of their total F_1/F_3 cross peak volumes in the 3D NOESY spectra. Total volumes were obtained by adding the volumes for a given cross peak in the two or three F_2 planes in which it appeared. Upper bounds for the NOE constraints obtained from the ^{1}H–^{15}N NOESY-HSQC spectrum were calibrated using volumes from NH/NH cross peaks corresponding to helical regions of the protein. Those obtained from the ^{1}H–^{13}C NOESY-HSQC spectrum were calibrated using ^{1}Hβ/^{1}Hβ distances for methylene groups. The resulting upper bound distance restraints were 2.7, 3.5, and 5.0 Å for backbone–backbone NOEs and 5.0 Å for NOEs involving side chain protons. Lower bounds between nonbonded atoms were set to the sum of their van der Waals radii. A total of 193 interresidue and 55 intraresidue distance restraints and 18 dihedral angle restraints were used for these preliminary distance geometry calculations. The dihedral angle restraints were determined from $^3J_{HN\alpha}$ coupling constants derived from a 2D HMQC-J spectrum (Kay & Bax, 1990) of uniformly ^{15}N-labeled GAL4(62). On the basis of the Cd coordination determined for $Cd(II)_2$GAL4 (Gadhavi et al., 1991; Gardner, et al., 1991), one of the two zinc atoms was constrained to be tetrahedrally coordinated by Cys 11, Cys 14, Cys 21, and Cys 28, and the other zinc was constrained to be tetrahedrally coordinated by Cys 11, Cys 28, Cys 31, and Cys 38. Two additional distance restraints were added between the sulfur atoms of Cys 21 and Cys 38, and between the sulfur atoms of Cys 14 and Cys 31, in order to maintain the planarity of the two tetrahedrons, i.e., the sulfur atoms of Cys 11 and Cys 28 and the two zinc atoms are coplanar. The chirality of the two tetrahedrons was determined in preliminary structure calculations carried out without these additional constraints. Pseudoatom corrections were added to interproton distance restraints where necessary (Wüthrich et al., 1983). In addition, six hydrogen-bond constraints identified on the basis of short- and medium-range backbone–backbone NOE connectivities and slow amide proton exchange were used in the helical regions of the protein. Structures were calculated on a Titan II computer using the distance geometry program DIANA (Güntert et al., 1991).

RESULTS

^{1}H and ^{15}N Backbone Assignments. Sequential assignment of the majority of backbone ^{1}H and ^{15}N resonances in the spectrum of GAL4(62) was achieved by combined use of homonuclear 2D and heteronuclear 2D and 3D experiments. Initial spin system assignments were obtained from 2D homonuclear DQF-COSY and TOCSY spectra. 2D ^{1}H–^{15}N HSQC-TOCSY and 3D ^{1}H–^{15}N TOCSY-HSQC were found to be useful in obtaining additional spin system assignments and in resolving ambiguities which were present in the 2D homonuclear spectra due to overlap of amide ^{1}H resonances. In addition, experiments involving specific ^{15}N labeling of Lys, Arg, and Leu residues, which together total almost 40% of the amino acids in GAL4(62), provided unambiguous identification of the backbone ^{1}H and ^{15}N resonances of these spin systems (data not shown). Identification of the two Ile residues and the unique Val 57 were straightforward in the DQF-COSY and the 3D ^{1}H–^{15}N TOCSY-HSQC spectra. Assignments of the three Ala residues and the three Thr residues were also readily achieved by use of the 2D ^{1}H–^{15}N HSQC-TOCSY and 3D ^{1}H–^{15}N TOCSY-HSQC spectra. Most of the AMX spin systems could be identified in the TOCSY, DQF-COSY, 2D ^{1}H–^{15}N HSQC-TOCSY, and/or 3D ^{1}H–^{15}N TOCSY-HSQC spectra. The aromatic proton resonances of the unique Trp 36 and Tyr 40 residues were previously identified by specific deuteration and NOE experiments (Serikawa et al., 1992). These assignments were confirmed by using the DQF-COSY and TOCSY experiments, and the ^{1}Hβ resonances were identified in the NOESY spectra from cross peaks involving the ring C2H resonance of Trp 36 and the ring C2,6H resonance of Tyr 40. Four out of seven Glu and Gln residues were identified from the 2D ^{1}H–^{15}N HSQC-TOCSY and the ^{15}N slices of the 3D ^{1}H–^{15}N TOCSY-HSQC spectra.

Sequential assignment of the backbone ^{1}H and ^{15}N resonances was completed in the conventional manner (Billeter et al., 1982; Wüthrich, 1986) by using mainly 2D ^{1}H–^{1}H NOESY and 2D ^{1}H–^{15}N HSQC-NOESY spectra to identify short-range NOEs connecting the previously identified spin systems. Examples indicating the sequential $d_{\alpha N}(i,i+1)$ connectivities observed for residues 10–19 and 27–41 in the 2D ^{1}H–^{1}H NOESY spectrum and sequential $d_{NN}(i,i+1)$ connectivities observed for residues 12–19 in the 2D ^{1}H–^{15}N HSQC-NOESY spectrum are given in Figures 1 and 2, respectively. Since ambiguity due to poor resolution in some parts of the spectrum remained, a 3D ^{1}H–^{15}N NOESY-HSQC spectrum of uniformly ^{15}N-labeled GAL4(62) was acquired. The latter spectrum, together with the 3D ^{1}H–^{15}N TOCSY-HSQC spectrum, was acquired using spin lock purge pulses to achieve solvent suppression, rather than presaturation, thus ensuring that NH/^{1}Hα connectivities were observed for both ^{1}Hα resonances close to the water peak and for the more rapidly exchanging NHs. Indeed, a number of peaks were observed in these spectra which were absent from spectra acquired using presaturation. The $d_{\alpha N}(i,i+1)$ sequential connectivities obtained in the 3D ^{1}H–^{15}N NOESY-HSQC spectrum for residues 56–59 are illustrated in Figure 3.

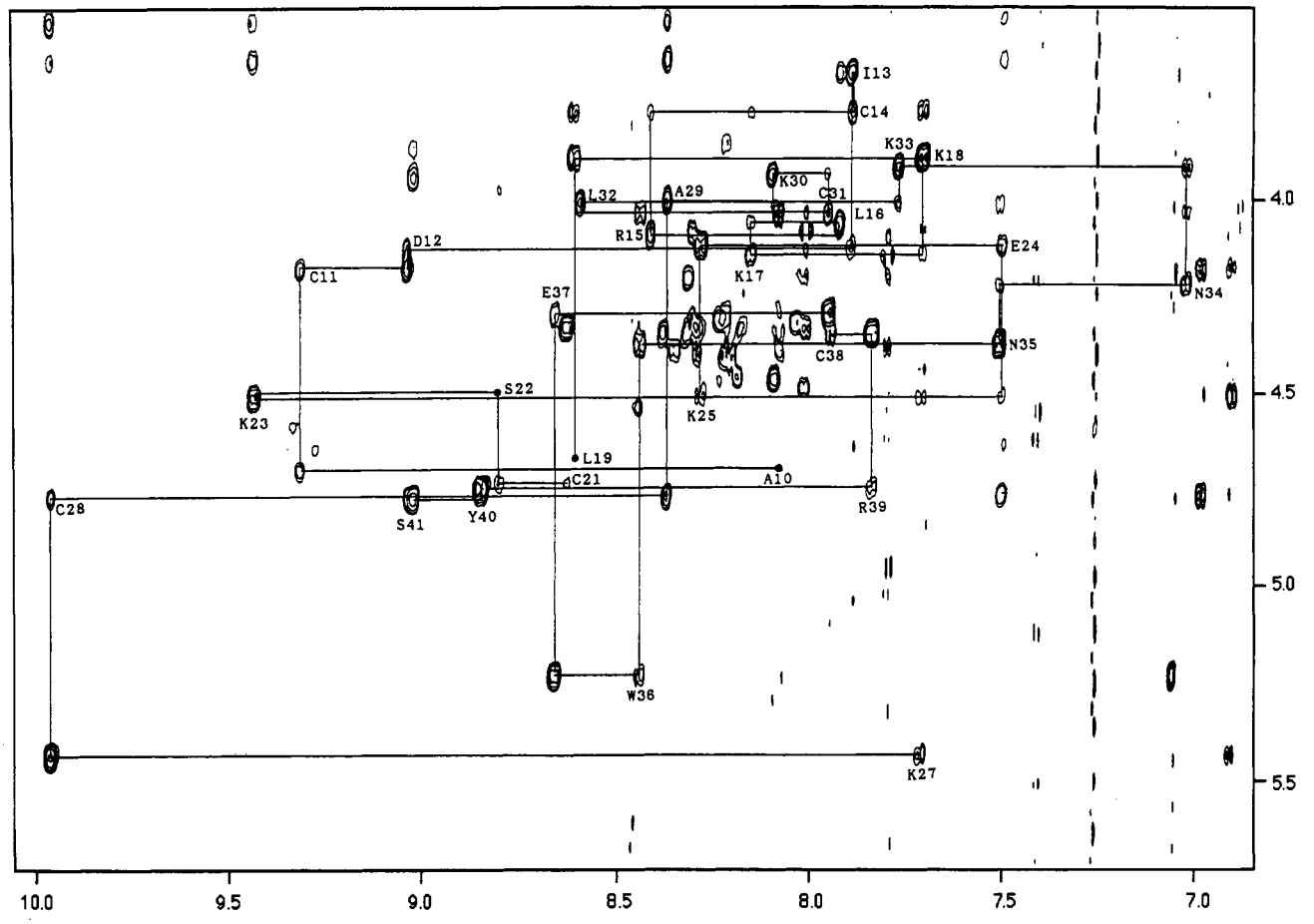

FIGURE 1: Section of the 600-MHz ^1H–^1H NOESY spectrum of GAL4(62) at 40 °C and pH 5.5. The mixing time was 100 ms. Sequential $d_{\alpha N}(i,i+1)$ connectivities for residues 10–19 and for residues 27–41 are indicated.

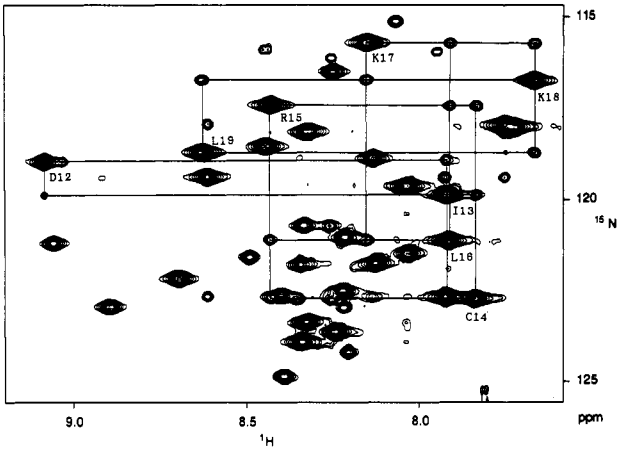

FIGURE 2: Section of the 600-MHz ^1H–^{15}N HSQC-NOESY spectrum of uniformly ^{15}N-labeled GAL4(62) at 30 °C and pH 5.6. The mixing time was 150 ms. Presaturation was used for solvent suppression. Sequential $d_{NN}(i,i+1)$ connectivities for residues 12–19 are indicated.

Sequential connectivities for other regions of the protein were also obtained or confirmed in the 3D experiment by observation of $d_{NN}(i,i+1)$, $d_{\alpha N}(i,i+1)$, and $d_{\beta N}(i,i+1)$ short-range and other medium-range NOEs.

The assignments of the ^1H and ^{15}N resonances obtained for GAL4(62) are indicated on the ^1H–^{15}N HSQC spectrum shown in Figure 4 and are listed in Table I. Six side chain amide proton resonances of the three Asn and Gln residues were also identified on the basis of intraresidue NOEs from $^1H\beta$ or $^1H\gamma$ and are indicated in Figure 4. Observed sequential and medium-range NOE connectivities are summarized in Figure 5.

Aliphatic ^1H and ^{13}C Assignments. At this stage all the polypeptide backbone ^1H and ^{15}N chemical shifts of GAL4-(62) were known, with the exceptions of Met 1, Lys 2, Glu 8, and the ^{15}N resonances of the prolines 26, 42 and 48. Sequential assignments of the $^{13}C\alpha$ resonances were then obtained by using a 3D constant-time triple-resonance HCA-(CO)N experiment (Palmer et al., 1992), which correlates the $^1H\alpha$ and $^{13}C\alpha$ chemical shifts of each residue with the amide ^{15}N chemical shift of the following residue in the protein.

A representative $F_1(^{13}C\alpha)/F_3(^1H\alpha)$ plane of the HCA-(CO)N spectrum, at the $F_2(^{15}N)$ chemical shift of 121.5 ppm (after allowing for the deuterium isotope shift) is shown in Figure 6. The $^1H\alpha$ chemical shifts of Ser 6, Gln 9, Arg 15, Cys 28, Tyr 40, Pro 42, and Pro 48 were previously determined, as discussed above, while the backbone ^{15}N chemical shifts of residues Ile 7, Ala 10, Leu 16, Ala 29, Ser 41, Lys 43, and Leu 49 were previously determined to be 121.5, 121.8, 121.1, 121.8, 121.2, 121.6, and 121.1 ppm, respectively (see Figure 4). Therefore, assignments of the $^{13}C\alpha$ resonances for residues 6, 9, 15, 28, 40, 42, and 48 can be made directly from the $F_1(^{13}C\alpha)/F_3(^1H\alpha)$ plane of the HCA(CO)N spectrum illustrated in Figure 6. Most assignments of the cross peaks in the HCA(CO)N spectrum of GAL4(62) to sequential pairs of residues were unambiguously obtained in a similar fashion. Since the backbone ^{15}N resonances of the three proline residues and of Glu 8 were not obtained from the previous 3D ^1H–^{15}N experiments, $^{13}C\alpha$ resonance assignments for Ile 7, Lys 25, Ser 41, and Ser 47 could not be obtained using this procedure.

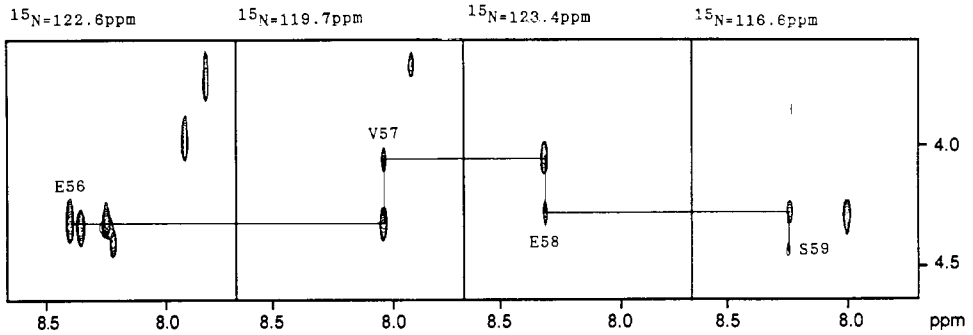

FIGURE 3: Selected regions from ^{15}N planes of the 600-MHz 3D ^{1}H–^{15}N NOESY-HSQC spectrum of uniformly ^{15}N-labeled GAL4(62) at 30 °C and pH 5.6. Sequential $d_{\alpha N}(i,i+1)$ connectivities for residues 56–59 are indicated.

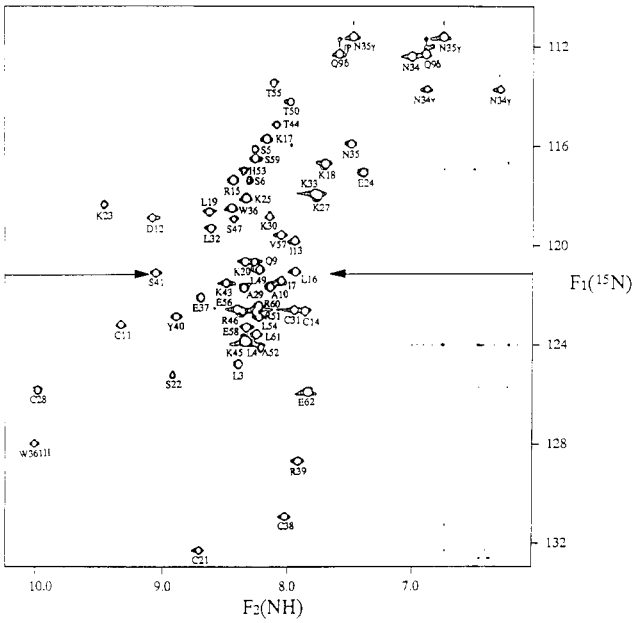

FIGURE 4: 600-MHz ^{1}H–^{15}N HSQC spectrum of uniformly ^{15}N-labeled GAL4(62) at 30 °C and pH 5.6, acquired using a spin lock pulse for solvent suppression. Cross peak assignments are indicated. The line at 121.5 ppm indicates the ^{15}N frequency corresponding to the $F_1(^{13}C\alpha)/F_3(^{1}H\alpha)$ plane of the HCA(CO)N spectrum shown in Figure 6.

Similarly, resonance assignments could not be obtained for Met 1 and Lys 2 without resort to the HCCH experiments, because no assignments were obtained for these residues from the 3D ^{1}H–^{15}N experiments. In addition, the C-terminal residue Glu 62 gives no cross peak in the HCA(CO)N experiment due to the lack of a following amide group.

With most of the backbone $^{13}C\alpha$ and $^{1}H\alpha$ chemical shifts determined using the 3D HCA(CO)N spectrum, it was possible to delineate the amino acid spin systems by combined use of the 3D constant-time HCCH-COSY (Ikura et al., 1991a) and HCCH-TOCSY (Bax et al., 1990b) spectra. For instance, since analysis of the 3D HCA(CO)N spectrum revealed the $^{13}C\alpha$ and $^{1}H\alpha$ chemical shifts of Pro 42 to be 60.8 and 4.54 ppm, respectively, and those of Pro 48 to be 61.3 and 4.44 ppm, respectively (Figure 6), it was possible to identify the $^{13}C\alpha/^{1}H\alpha$ cross peaks of Pro 42 and Pro 48 in the appropriate $F_1(^{1}H)/F_3(^{1}H)$ plane of the 3D HCCH-TOCSY spectrum of GAL4(62) [i.e., at $F_2(^{13}C)$ chemical shift ~61.0 ppm] together with their accompanying side chain protons (Figure 7A). The $^{1}H\beta$ resonances are easily distinguished by comparison with the $F_1(^{1}H)/F_3(^{1}H)$ plane at the same $F_2(^{13}C)$ frequency in the 3D HCCH-COSY spectrum (Figure 7B). Following identification of the $F_2(^{13}C\alpha)$ planes and their associated $^{1}H/^{1}H$ cross peaks in the HCCH-TOCSY and HCCH-COSY spectra, the remaining aliphatic ^{13}C and ^{1}H resonances were assigned by identification of the same $^{1}H/^{1}H$ cross peak patterns in the appropriate $F_2(^{13}C)$ planes (Clore et al., 1990; Ikura et al., 1991b; Pelton et al., 1991; Fairbrother et al., 1992). For example, Figure 8 illustrates several $F_1(^{1}H)/F_3(^{1}H)$ planes from the 3D HCCH-TOCSY spectrum at $F_2(^{13}C)$ frequencies corresponding to $^{13}C\alpha$, $^{13}C\beta$, $^{13}C\gamma$, $^{13}C\delta$, and $^{13}C\epsilon$ resonances of Lys 17. Using this approach, the chemical shifts of most of the aliphatic ^{1}H and ^{13}C resonances were readily obtained and are listed in Table I.

Comparison of the amino acid spin systems identified in the HCCH experiments with the previously determined (partial) assignments of $^{1}H\alpha$ and side chain ^{1}H resonances of Ile 7, Lys 25, Ser 41, Ser 47, and Glu 62 allowed unambiguous sequence specific assignment of these residues in the HCCH spectra. Therefore, since the $^{13}C\alpha$ and $^{1}H\alpha$ chemical shifts of these residues were now known, the corresponding cross peaks could be identified in the 3D HCA(CO)N spectrum, leading to assignment of the ^{15}N resonances of Glu 8, Pro 26, Pro 42, and Pro 48 (Table I).

The remaining incompletely assigned residues then were Met 1, Lys 2, and Glu 8. Assignments for Glu 8 were obtained by combined use of the appropriate $F_1(^{13}C\alpha)/F_3(^{1}H\alpha)$ slice of the HCA(CO)N spectrum [i.e., at the $F_2(^{15}N)$ frequency of Gln 9; 120.7 ppm] and spin system identification using the HCCH experiments. Assignments for the only methionine in the protein, Met 1, were easily obtained by identification of the spin system in the HCCH spectra. The backbone ^{15}N chemical shift of Lys 2 was found by identifying the $F_2(^{15}N)$ slice in the HCA(CO)N spectrum containing the $F_1(^{13}C\alpha)/F_3(^{1}H\alpha)$ cross peak corresponding to Met 1. The $F_1(^{13}C\alpha)/F_3(^{1}H\alpha)$ cross peak due to Lys 2 was found in the plane corresponding to the $F_2(^{15}N)$ chemical shift of Leu 3. The side chain assignments of Lys 2 could not be obtained from the HCCH spectra due to resonance degeneracy.

Amide Proton Exchange. In order to determine the amide proton exchange rates of individual residues, ^{1}H–^{15}N HSQC spectra were acquired following dissolution of uniformly ^{15}N-labeled GAL4(62) in D_2O. The protein was lyophilized once from H_2O at pH 5.5 and then dissolved in D_2O. ^{1}H–^{15}N HSQC spectra were acquired at 30 °C starting 7, 90, and 180 min following dissolution; each spectrum required 80 min of acquisition time. Only 18 cross peaks remained in the spectrum acquired starting 7 min after dissolution of the protein in D_2O. Ten more cross peaks were absent from the 90-min spectrum, and only six peaks remained in the spectrum acquired starting 180 min following dissolution. These data are summarized in Figure 5 and clearly show that exchange of most of the amide protons of GAL4(62) is rather rapid.

Secondary Structure. The pattern of sequential and medium-range NOEs shown in Figure 5, together with the observed groupings of slow amide proton exchange, suggests

Table I: ^{1}H, ^{15}N, and ^{13}C Chemical Shifts for GAL4(62) at pH 5.5 and 30 °C[a]

residue	^{15}N	NH	$^{13}C\alpha$	$^{1}H\alpha$	$^{13}C\beta$	$^{1}H\beta$	$^{13}C\gamma$	$^{1}H\gamma$	other ^{13}C	other ^{1}H	other ^{15}N
Met 1			52.8	4.12	30.6	2.15	28.2	2.57			
Lys 2	124.6		54.1	4.38							
Leu 3	124.8	8.39	52.7	4.39		1.60				δ 0.90	
Leu 4	123.9	8.35	52.9	4.40	40.1	1.61	24.7	1.61	δ 22.2	δ 0.90	
Ser 5	116.2	8.26	56.1	4.46	62.0	3.86					
Ser 6	117.5	8.30	56.2	4.48	62.0	3.87					
Ile 7	121.5	8.04	59.2	4.19	36.4	1.85	24.7 (15.2)[b]	1.41, 1.13 (0.82)	δ 10.3	δ 0.79	
Glu 8	123.9		54.4	4.30	27.7	2.06, 1.96	33.9	2.26			
Gln 9	120.7	8.26	53.3	4.45	27.7	2.19, 2.05	31.1	2.49		ε 7.57, 6.88	ε 112.4
Ala 10	121.8	8.13	49.4	4.65	18.7	1.53					
Cys 11	123.3	9.31	55.8	4.17	28.7	2.92, 2.19					
Asp 12	119.0	9.06	55.8	4.11	37.9	2.59					
Ile 13	119.9	7.93	62.2	3.68	34.9	1.79	26.7 (16.7)	1.50, 0.95 (0.61)	δ 9.3	δ 0.63	
Cys 14	122.7	7.85	63.4	3.78	26.7	3.22, 2.78					
Arg 15	117.5	8.42	57.4	4.07	27.7	1.90, 1.82	25.2	1.55	δ 41.6	δ 3.31, 3.19	
Leu 16	121.1	7.92	55.8	4.04	40.1	1.77, 1.72	24.7	1.62	δ 21.7	δ 0.84	
Lys 17	115.8	8.16	54.4	4.11	30.6	1.93, 1.58	23.7	1.32	δ 26.7; ε 39.6	δ 1.44, 1.21; ε 2.43, 2.27	
Lys 18	116.8	7.68	55.1	3.89	25.9	2.13, 1.86	22.2	1.35	δ 26.7; ε 39.8	δ 1.70; ε 3.02	
Leu 19	118.7	8.62	50.5	4.64	42.6	1.87, 1.48	24.2	1.57	δ 23.4; 19.7	δ 1.07, 0.89	
Lys 20	120.7	8.33	53.8	4.34	30.6	1.83, 1.75	22.2	1.44	δ 26.7; ε 39.6	δ 1.68; ε 3.00	
Cys 21	132.3	8.70	58.6	4.70	30.1	2.89					
Ser 22	125.3	8.91	58.1	4.49	61.0	4.33, 3.98					
Lys 23	118.5	9.44	55.9	4.52	26.7	2.01, 1.97	22.9	1.41	δ 27.2; ε 40.1	δ 1.59, 1.50; ε 2.97, 2.90	
Glu 24	117.1	7.37	55.1	4.11	29.6	1.99	35.1	2.34, 2.24			
Lys 25	118.2	8.33	50.2	4.51	30.6	1.55, 1.70	22.2	1.21	δ 26.2; ε 39.1	δ 1.32; ε 2.40, 2.04	
Pro 26	133.1		62.1	4.45	35.4	2.52, 2.21	22.7	2.05, 1.86	δ 48.0	δ 3.77, 3.45	
Lys 27	118.1	7.74	52.5	5.43	35.4	1.64	23.2	1.52	δ 27.7; ε 40.1	δ 1.72, 1.61; ε 3.05	
Cys 28	125.9	9.98	55.3	4.70	29.6	3.65, 3.55					
Ala 29	121.8	8.34	53.4	4.00	16.0	1.50					
Lys 30	118.9	8.14	56.7	3.94	30.1	2.03, 1.94	22.7	1.54	δ 26.2; ε 39.8	δ 1.69; ε 3.06, 3.00	
Cys 31	122.7	7.93	62.4	4.02	27.0	3.30, 2.80					
Leu 32	119.4	8.60	55.6	3.99	40.1	1.72, 1.51	24.2	1.50	δ 22.2	δ 0.88	
Lys 33	118.0	7.76	56.1	3.90	29.9	1.80, 1.67	22.2	1.34	δ 26.2; ε 39.6	δ 1.59; ε 2.91	
Asn 34	112.5	6.98	51.0	4.18	35.4	1.17, 0.58				δ 6.87, 6.29	δ 113.7
Asn 35	116.0	7.47	52.0	4.38	34.4	3.16, 2.66				δ 7.45, 6.74	δ 111.7
Trp 36	118.6	8.43	51.2	5.20	30.1	3.39, 3.17				δ1 6.99; ε3 8.04; ζ3 6.83; η2 7.04; ζ2 7.37; ε1 10.01	ε1 128.0
Glu 37	122.2	8.68	53.8	4.29	26.2	1.97, 1.92	33.6	2.25, 2.17			
Cys 38	131.0	8.02	60.2	4.33	28.7	3.10, 2.58					
Arg 39	128.7	7.90	52.5	4.70	31.4	1.72	24.7	1.56	δ 41.1	δ 3.23, 3.17	
Tyr 40	122.9	8.88	54.9	4.73	36.6	2.83, 2.76				δ 6.92; ε 6.86	
Ser 41	121.2	9.03	55.7	4.73	60.5	3.91, 3.84					
Pro 42	137.2		60.8	4.54	29.6	2.32, 1.95	24.7	2.05	δ 48.5	δ 3.90, 3.75	
Lys 43	121.6	8.48	54.5	4.30		1.80		1.47		δ 1.73; ε 3.00	
Thr 44	115.2	8.07	59.5	4.32	67.9	4.16	18.7	1.20			
Lys 45	123.9	8.35	54.1	4.32				1.95		ε 3.00	
Arg 46	122.7	8.35	53.6	4.37	28.7	1.86, 1.75	24.7	1.63	δ 41.1	δ 3.19	
Ser 47	119.0	8.42	54.2	4.75	61.5	3.85					
Pro 48	138.1		61.3	4.44	29.6	2.30, 1.93	24.7	2.01	δ 48.5	δ 3.83, 3.75	
Leu 49	121.1	8.21	53.4	4.35		1.62		1.62		δ 0.87	
Thr 50	114.3	7.96	59.7	4.31	67.9	4.21	18.7	1.20			
Arg 51	122.7	8.24	54.0	4.31	28.2	1.85, 1.74	24.7	1.62	δ 41.1	δ 3.19	
Ala 52	124.2	8.20	50.5	4.21	16.7	1.31					
His 53	117.1	8.42	53.3	4.65	26.7	3.25, 3.16				δ2 7.23; ε1 8.47	
Leu 54	122.9	8.23	53.3	4.38		1.62		1.62		δ 0.87	
Thr 55	113.5	8.11	59.7	4.33	67.9	4.26	18.7	1.18			
Glu 56	122.6	8.40	54.8	4.32		2.07		2.27			
Val 57	119.7	8.04	60.5	4.05	30.1	2.07	18.2	0.92			
Glu 58	123.4	8.32	54.7	4.27	33.6	2.26, 1.98	33.6	2.26			
Ser 59	116.6	8.25	56.3	4.41	62.0	3.83					
Arg 60	122.5	8.22	53.8	4.39	28.7	1.87, 1.77	24.7	1.60	δ 41.1	δ 3.19	
Leu 61	123.6	8.24	53.0	4.37		1.47	24.7	1.61	δ 21.0	δ 0.87	
Glu 62	125.9	7.82	55.5	4.11	28.7	1.88	33.9	2.19			

[a] Uncertainties are ±0.05, 0.1, and 0.2 ppm for ^{1}H, ^{15}N, and ^{13}C, respectively, except for proline ^{15}N chemical shifts, which have an uncertainty of ±0.2. [b] Values in parentheses correspond to Ile $C\gamma H_3$.

the presence of two α-helices (Wüthrich, 1986) in GAl4(62), from residue Asp 12 to Leu 19 and from residue Lys 30 to Trp 36. These two helices are in locations identical to those identified by Gadhavi et al. (1990) in a smaller fragment of the GAL4 DNA-binding domain encompassing residues 7–49.

The ^{13}C chemical shifts also contain valuable information regarding protein secondary structure (Spera & Bax, 1991; Wishart et al., 1991; Ikura et al., 1991b). Figure 9 shows secondary shift differences between the $^{13}C\alpha$ chemical shifts of each amino acid residue in GAL4(62) and their random-coil shifts. The positions of α-helices as identified from NOE and amide proton exchange data are also indicated. There is a clear correlation between $^{13}C\alpha$ chemical shifts and the two helical regions of GAL4(62) consistent with the observations of Spera and Bax (1991) and of Wishart et al. (1991). For the five residues located at the N-terminal end of the two

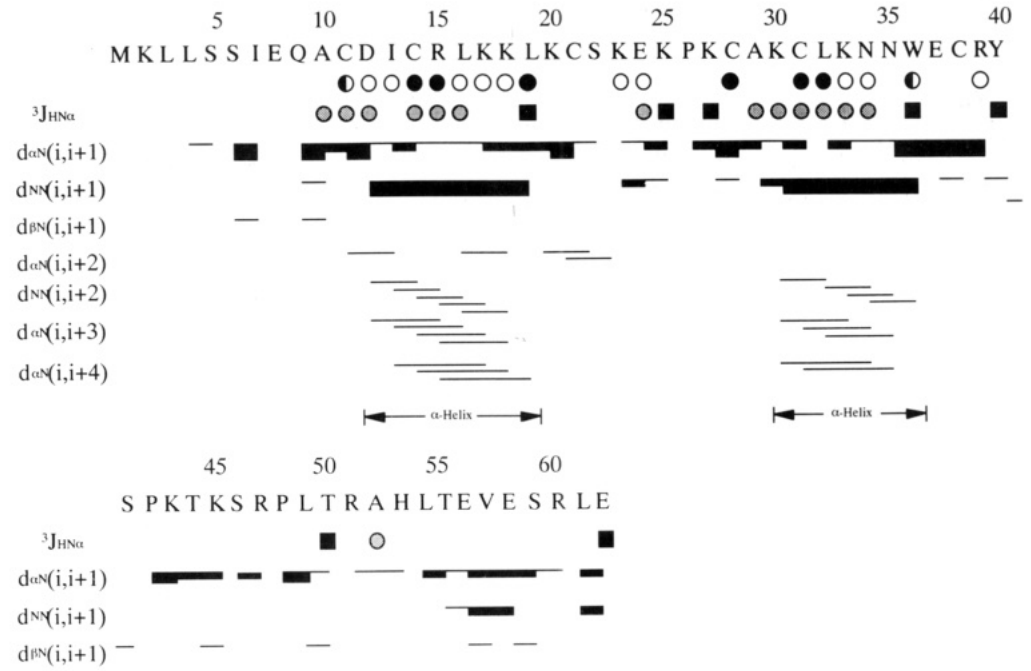

FIGURE 5: Summary of the sequential NOE connectivities observed for GAL4(62). Sequential NOEs are represented by bars, the size of which indicated the NOE intensity (strong, medium, and weak). Amide protons that exchange slowly are indicated. (Open circles) Lifetime greater than 7 min but less than 90 min. (Solid semicircles) Lifetime greater than 90 min but less than 180 min. (Solid circles) Lifetime greater than 180 min. $^3J_{HN\alpha}$ coupling constants less than 5.5 Hz are indicated by shaded circles while those greater than 8.5 Hz are indicated by solid boxes.

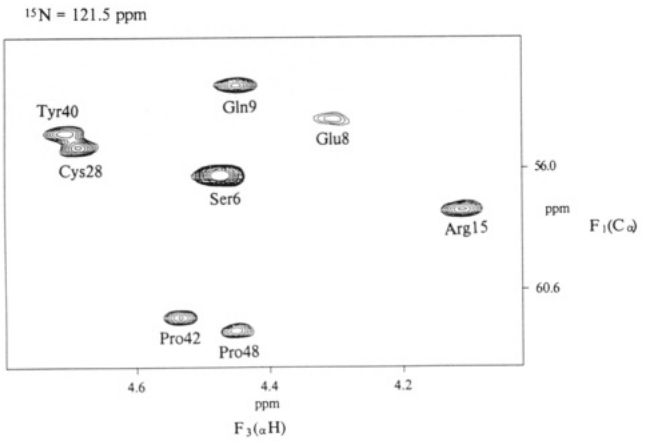

FIGURE 6: Representative $F_1(^{13}C\alpha)/F_3(^1H\alpha)$ plane, at $F_2(^{15}N)$ = 121.5 ppm, of the 500 MHz 3D constant-time HCA(CO)N spectrum of uniformly $^{15}N/^{13}C$-labeled GAL4(62). Residues numbers indicate $^{13}C\alpha(i)/^1H\alpha(i)/^{15}N(i+1)$ cross peaks.

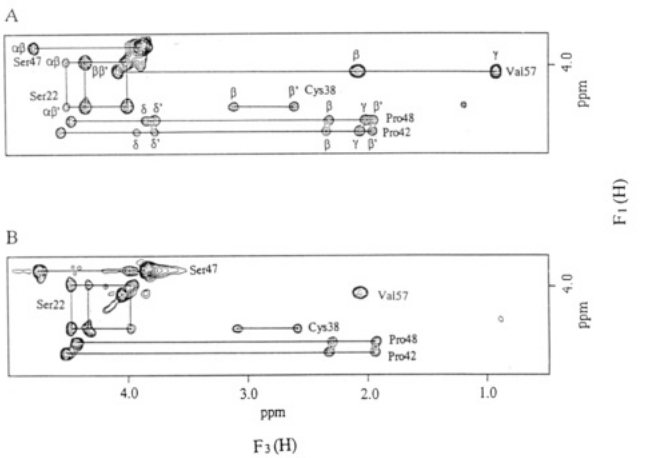

FIGURE 7: Selected slices at $F_2(^{13}C)$ = 29.2 ppm for positive peaks, and 61.0 ppm for negative peaks, of the 500-MHz HCCH-TOCSY (A) and constant-time HCCH-COSY (B) spectra of uniformly $^{15}N/^{13}C$-labeled GAL4(62), illustrating connectivities originating from the $^1H\alpha$ of Cys 38, Pro 42, Pro 48, and Val 57 and from the $^1H\beta$ of Ser 22 and Ser 47.

α-helices (12–16 and 29–33), the $^{13}C\alpha$ resonates downfield relative to the random-coil shifts. The $^{13}C\alpha$ of the residues located at the C-terminal ends of the putative helices, Leu 19 and Trp 36, however, resonate significantly upfield, indicating that these residues are not in a helical conformation. The recently published ϕ and ψ dihedral angles for the solution structure of GAL4(65) (Baleja et al., 1992) are entirely consistent with the observed secondary shift in the case of Trp 36 but are inconsistent in the case of Leu 19 (Spera & Bax, 1991) [We note, however, that the uncertainty in the ψ angle quoted for Leu 19 was greater than 60° (Baleja et al., 1992)]. In the published solution and crysal structures of GAL4(65) (Baleja et al., 1992; Marmorstein et al., 1992), residues Lys 18 and Asn 35 were identified as having positive ϕ angles. The small downfield shift of the $^{13}C\alpha$ resonances for these residues is also consistent with the observations of Spera and Bax (1991).

The N-terminal (residues 1–9) and C-terminal (residues 41–62) regions of the protein appear devoid of any regular secondary structure and are probably flexible in solution, on the basis of the observed small chemical shift dispersion, the weak sequential NOE connectivities, and rapid amide proton exchange (Figure 5 and 9, Table I). These conclusions are also consistent with the solution state studies of Kraulis et al. (1992) and of Baleja et al. (1992).

Structures of GAL4(62). The assignments discussed above have allowed preliminary analysis of 3D $^1H-^{15}N$ NOESY-HSQC and $^1H-^{13}C$ NOESY-HSQC spectra of GAL4(62), from which a subset of NOEs were identified. A total of 10 distance geometry (DG) structures were calculated for residues 10–40, using the distance and dihedral angle restraints described under Materials and Methods. The nine N-terminal and 22 C-terminal residues were omitted from the calculation

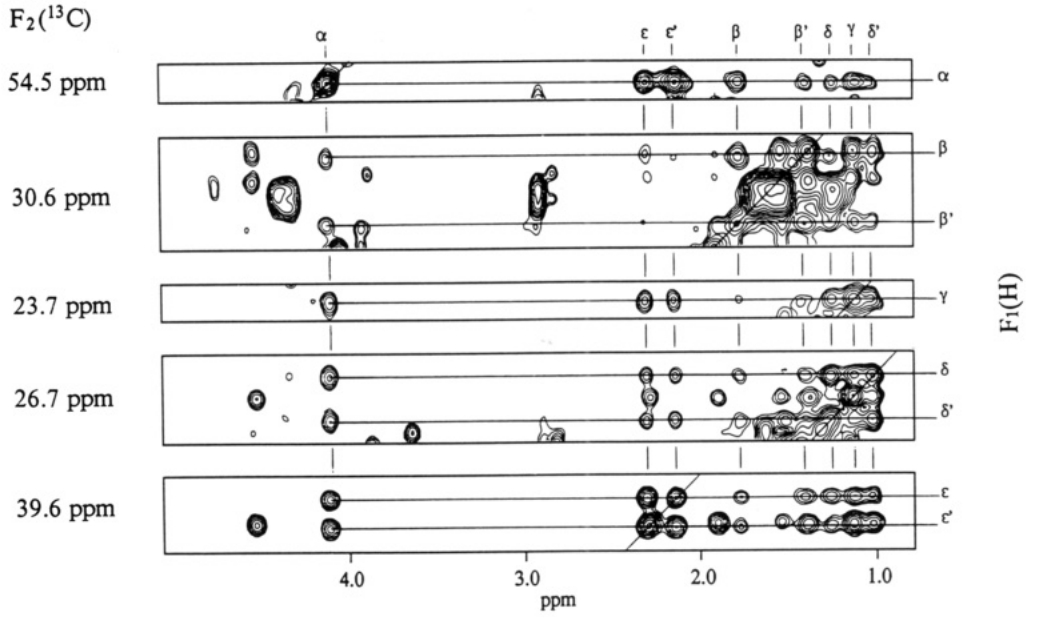

FIGURE 8: Selected slices at different $F_2(^{13}C)$ chemical shifts of the 23.1-ms mixing time 3D HCCH-TOCSY spectrum of uniformly $^{15}N/^{13}C$-labeled GAL4(62), illustrating connectivities originating from the $^1H\alpha$, $^1H\beta$, $^1H\gamma$, $^1H\delta$, and $^1H\epsilon$ of Lys 17.

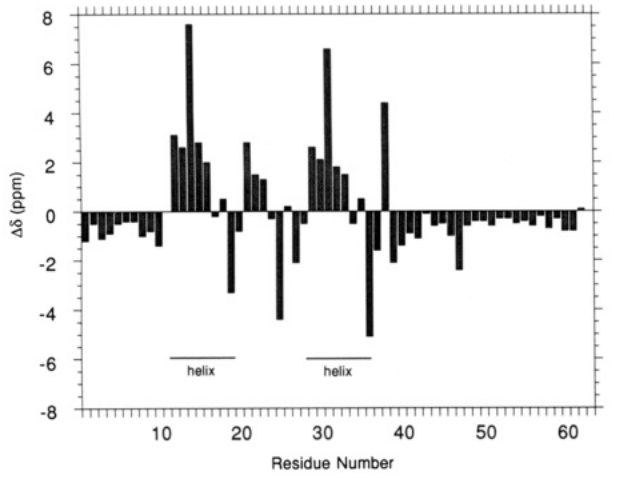

FIGURE 9: Plot of the differences between the $^{13}C\alpha$ chemical shifts of each amino acid residue in GAL4(62) and the random coil shifts (Richarz & Wüthrich, 1978). The random coil $^{13}C\alpha$ chemical shift for reduced Cys was taken to be 55.8 ppm (Howarth & Lilley, 1978). The location of the two α-helices as deduced from NOE connectivities is also shown.

because, as discussed above, they appear to be disordered in solution. A schematic illustration of the DG structure having the lowest target function value is shown in Figure 10. The average backbone RMS deviation of the 10 calculated structures is 1.34 Å. The overall structure comprises two similar segments, each of which consists of a short helix, a sharp turn, and an extended structure. The individual segments are linked by the two ligating zinc atoms and a short loop and are related to each other by a 2-fold pseudosymmetry axis (Figure 10). While we have not compared the coordinates of our preliminary model of the DNA-binding domain of GAL4 with those of the recently published solution structures (Kraulis et al., 1992; Baleja et al., 1992), it is clear that the overall folds are similar. We anticipate that the additional spectral assignments obtained in the current study, relative to the recently published work, will allow a large number of NOE connectivities to be unambiguously assigned and hence result in a larger number of distance restraints and consequently a higher resolution structure.

DISCUSSION

Most of the ^1H, aliphatic ^{13}C, and ^{15}N chemical shifts of GAL4(62) have now been obtained from a combined analysis of 3D triple-resonance HCA(CO)N, double-resonance HCCH-COSY, HCCH-TOCSY, TOCSY-HSQC, NOESY-HSQC, and a number of other 2D homonuclear and heteronuclear NMR techniques. The ^1H resonance assignments of an almost identical GAL4 fragment, GAL4(62*), were also reported recently (Pan & Coleman, 1991; Gardner et al., 1991). Although their assignments for the regions Cys 14–Leu 19 and Pro 26–Thr 44 are in good agreement with our own (after accounting for an approximately 0.05 ppm systematic difference in the chemical shifts due probably to temperature differences between the two studies), there are a number of significant differences in other regions of the protein. In contrast to this result, the agreement between assignments reported for the smaller GAL4(7–47) fragment (Gadhavi et al., 1990) and those reported here is generally good. Most of our sequential assignments were checked by using the HCA(CO)N experiment, which gives sequential connectivities via scalar couplings, as well as by the more conventional through-space dipolar couplings observed in homonuclear 2D and heteronuclear 2D and 3D NOESY spectra.

Information on the secondary structure of GAL4(62) could be obtained from an analysis of the $^{13}C\alpha$ chemical shift data, as well as the pattern of short- and medium-range NOEs observed and the qualitative amide proton exchange rates. With the exception of Leu 19, the secondary shift differences between the $^{13}C\alpha$ chemical shifts for residues 12–19 and 29–36 (i.e., the "helical" regions of the protein) and random-coil values are consistent with the recently published ϕ and ψ dihedral angles of GAL4(65) (Baleja et al., 1992), according to the correlations of Spera and Bax (1991). Indeed, the $^{13}C\alpha$ chemical shifts give a clearer indication that the α-helices include only residues 12–17 and 29–34 (Baleja et al., 1992) than the pattern of sequential and medium range NOEs, which considered alone suggest that the helices include residues 12–19 and 30–36. A similar observation was recently made regarding the start of the α-helix and in the zinc-finger peptide Xfin-31, for which it was concluded that the chemical shifts appeared more sensitive to the ϕ and ψ dihedral angles than

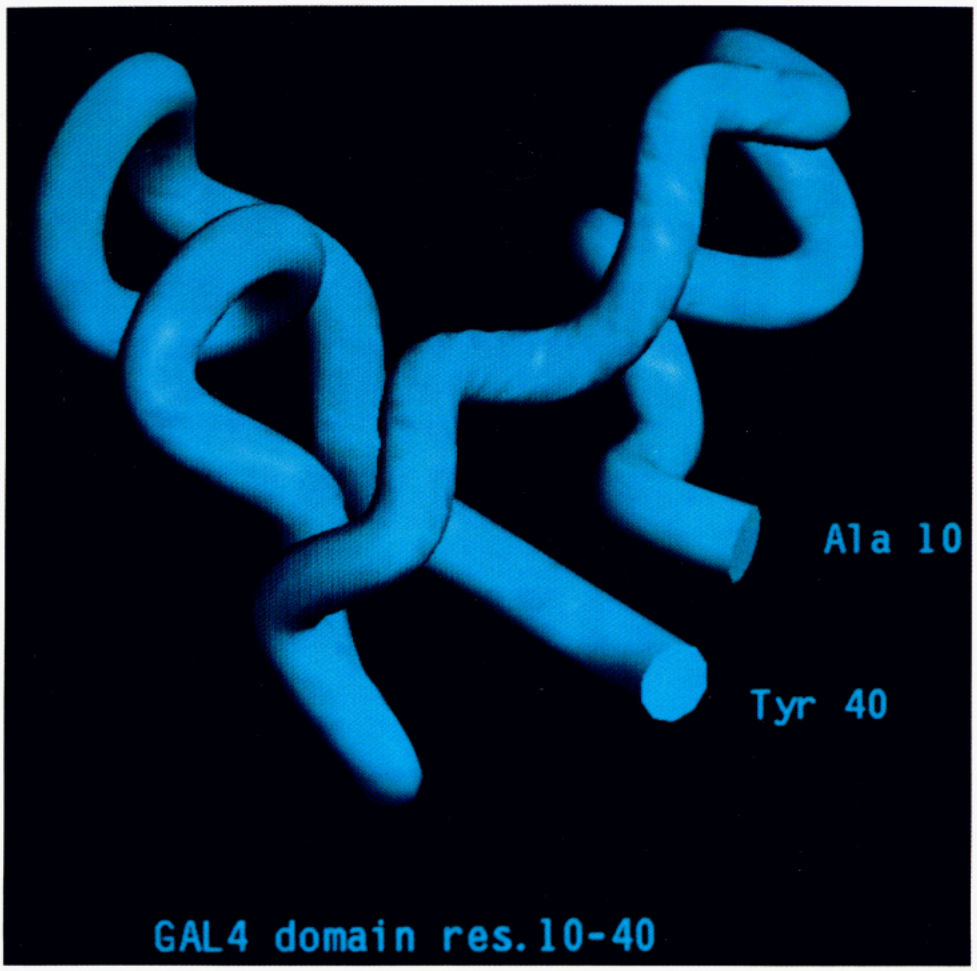

FIGURE 10: Schematic diagram illustrating the fold calculated for residues 10–40 of the DNA-binding domain of GAL4(62).

the medium-range NOEs (Lee et al., 1992). On the basis of both the observed NOE connectivities and chemical shifts, residues 1–9 and 41–62 appear to be unstructured and flexible in solution. There is no evidence for any secondary structure formation in the region following residue 50 where a coiled-coil dimerization motif is observed in the X-ray crystal structure of a GAL4(65)–DNA complex (Marmorstein et al., 1992).

It is also noted that the $^{13}C\alpha$ resonances of four out of the six Cys residues (14, 21, 31, and 38), which are the nonbridging ligands to Zn(II) (Gadhavi et al., 1991; Gardner et al., 1991), have unusually low-field chemical shifts relative to random-coil shifts (ca. +3 ppm; Figure 9). For Cys 14 and Cys 31 this effect appears to be additive with the downfield shift resulting from the helical conformation of these residues. The remaining two Cys residues, 11 and 28, are bridging ligands in the $Zn(II)_2$GAL4(62) binuclear cluster (Gadhavi et al., 1991; Gardner et al., 1991) and exhibit no significant shifts of their $^{13}C\alpha$ resonances.

In addition the $^{13}C\beta$ and $^{13}C\gamma$ chemical shifts of Pro 26, which has been identified as a *cis*-proline (Marmorstein et al., 1992; Kraulis et al., 1992; Baleja et al., 1992), are about 5 ppm downfield and 2 ppm upfield, respectively, of the corresponding shifts for the *trans*-Pro residues 42 and 48. This is consistent with the previous observations of Howarth and Lilley (1978) made using model peptides and the observation of a $^1H\alpha/^1H\alpha$ sequential NOE between Lys 25 and Pro 26 in the 3D ^1H–^{13}C NOESY-HSQC spectrum.

The ^1H, ^{13}C, and ^{15}N assignments reported here have been used in a partial analysis of 3D ^1H–^{15}N NOESY-HSQC and ^1H–^{13}C NOESY-HSQC spectra and have enabled the calculation of a preliminary solution structure for the globular domain of $Zn(II)_2$GAL4(62). The structure thus obtained is in good general agreement with the independently determined solution structures of $Zn(II)_2$GAL4(7–49) (Kraulis et al., 1992) and of $Cd(II)_2$GAL4(65) (Baleja et al., 1992). Refinement of the solution structure by addition of further distance restraints derived from the 3D heteronuclear edited NOESY spectra is currently in progress. In addition to the structural studies, the assignments obtained here will enable a study of the dynamics of the GAL4 DNA-binding domain to be carried out by analysis of ^{15}N and ^{13}C relaxation parameters.

REFERENCES

Andre, B. (1990) *Mol. Gen. Genet. 220*, 269–276.

Baleja, J. D., Marmorstein, R., Harrison, S. C., & Wagner, G. (1992) *Nature 356*, 450–453.

Bax, A., & Subramanian, S. J. (1986) *J. Magn. Reson. 67*, 565–569.

Bax, A., Ikura, M., Kay, L. E., Torchia, D. A., & Tschudin, R. (1990a) *J. Magn. Reson. 36*, 304–318.

Bax, A., Clore, M., & Gronenborn, A. M. (1990b) *J. Magn. Resoln. 88*, 425–431.

Bax, A., Ikura, M., Kay, L. E., & Guang, Z. (1991) *J. Magn. Reson. 91*, 174–178.

Billeter, M., Braun, W., & Wüthrich, K. (1982) *J. Mol. Biol. 155*, 321–346.

Bodenhausen, G., Ruben, D. J. (1980) *Chem. Phys. Lett. 69*, 185–189.

Borden, K. L. B., Bauer, C. J., Frenkiel, T. A., Beckmann, P., & Lane, A. N. (1992) *Eur. J. Biochem. 204*, 137–146.
Carr, M. D., Birdsall, B., Frenkiel, T. A., Bauer, C. J., Jimenez-Barbero, J., Polshakov, V. I., McCormick, J. E., Roberts, G. C. K., & Feeney, J. (1991) *Biochemistry 30*, 6330–6341.
Clore, G. M., Bax, A., Driscoll, P. C., Wingfield, P. T., Gronenborn, A. M. (1990) *Biochemistry 29*, 8172–8184.
Clubb, R. T., Thanabal, V., Osborne, C., & Wagner, G. (1991) *Biochemistry 30*, 7718–7730.
Driscoll, P. C., Clore, G. M., Marion, D., Wingfield, P. T., & Gronenborn, A. M. (1990) *Biochemistry 29*, 3542–3556.
Fairbrother, W. J., Cavanagh, J., Dyson, H. J., Palmer, A. G., Sutrina, S. L., Reizer, J., Saier, M. H., & Wright, P. E. (1991) *Biochemistry 30*, 6896–6907.
Fairbrother, W. J., Palmer, A. G., Rance, M., Reizer, J., Saier, M. H., & Wright, P. E. (1992) *Biochemistry 31*, 4413–4425.
Gadhavi, P. L., Raine, A. R. C., Alefounder, P. R., & Laue, E. D. (1990) *FEBS Lett. 276*, 49–53.
Gadhavi, P. L., Davis, A. L., Povey, J. F., Keeler, J., & Laue, E. D. (1991) *FEBS Lett. 281*, 223–226.
Gardner, K. H., Pan, T., Narula, S., Rivera, E., & Coleman, J. E. (1991) *Biochemistry 30*, 11292–11302.
Giniger, E., Varnum, M. S., & Ptashne, M. (1985) *Cell 40*, 767–774.
Güntert, P., Braun, W., & Wüthrich, K. (1991) *J. Mol. Biol. 217*, 517–530.
Howarth, O. W., & Lilley, D. M. J. (1978) *Prog. Nucl. Magn. Reson. Spectrosc. 12*, 1–40.
Ikura, M., Kay, L. E., & Bax, A. (1991a) *J. Biomol. NMR 1*, 299–304.
Ikura, M., Spera, S., Barbato, G., Kay, L. E., Krinks, M., & Bax, A. (1991b) *Biochemistry 30*, 9216–9228.
Kay, L. E., & Bax, A. (1990) *J. Magn. Reson. 86*, 110–126.
Kraulis, P., Raine, A. R. C., Gadhavi, P. L., & Laue, E. D. (1992) *Nature 356*, 448–450.
Laughon, A., & Gesteland, R. F. (1984) *Proc. Natl. Acad. Sci. U.S.A. 79*, 6827–6831.
Lee, M. S., Palmer, A. G., III, & Wright, P. E. (1992) *J. Biomol. NMR 2*, 307–322.
Ma, J., & Ptashne, M. (1987) *Cell 48*, 847–853.
Marion, D., & Wüthrich, K. (1983) *Biochem. Biophys. Res. Commun. 113*, 967–976.
Marion, D., Ikura, M., Tschudin, R., & Bax, A. (1989a) *J. Magn. Reson. 85*, 393–399.
Marion, D., Ikura, M., & Bax, A. (1989b) *J. Magn. Reson. 84*, 425–430.
Marmorstein, R., Carey, M., Ptashne, M., & Harrison, S. C. (1992) *Nature 356*, 408–414.
Miki, T., Yasukochi, T., Nagatani, H., Furuno, M., Orita, T., Yamada, H., Imoto, T., & Horiuchi, T. (1987) *Protein Eng. 1*, 327–332.
Messerle, B. A., Wider, G., Otting, G., Weber, C., & Wüthrich, K. (1989) *J. Magn. Reson. 85*, 608–613.
Norwood, T. J., Boyd, J., Heritage, J. E., Soffe, N., & Campbell, I. D. (1990) *J. Magn. Reson. 87*, 488–501.
Oshima, Y. (1981) in *Molecular Biology of the Yeast Saccharomyces* (Strathem, J., Jones, E., & Broach, J. K., Eds.) Vol. 1, pp 159–180, Cold Spring Harbor Lab, Cold Spring Harbor, NY.
Palmer, A. G., III, Fairbrother, W. J., Cavanagh, J., Wright, P. E., & Rance, M. (1992) *J. Biomol. NMR 2*, 103–108.
Pan, T., & Coleman, J. E. (1990a) *Biochemistry 29*, 3023–3029.
Pan, T., & Coleman, J. E. (1990b) *Proc. Natl. Acad. Sci. U.S.A. 87*, 2077–2081.
Pan, T., & Coleman, J. E. (1991) *Biochemistry 30*, 4212–4222.
Pelton, J. G., Torchia, D. A., Meadow, N. D., Wong, C.-Y., & Roseman, S. (1991) *Biochemistry 30*, 10043–10057.
Redfield, A. G., & Kunz, S. D. (1975) *J. Magn. Reson. 19*, 250–254.
Redfield, C., Smith, L. J., Boyd, J., Lawrence, G. M. P., Edwards, R. G., Smith, R. A. G., & Dobson, C. M. (1991) *Biochemistry 30*, 11029–11035.
Rhodes, D., & Klug, A. (1988) in *Nucleic Acids and Molecular Biology* (Eckstein, F., & Lilley, D. M. J., Eds.) Vol. 2, pp 149–166, Springer-Verlag, Berlin and Heidelberg.
Richarz, R., & Wüthrich, K. (1978) *Biopolymers 17*, 2133–2141.
Rucker, S. P., & Shaka, A. J. (1989) *Mol. Phys. 68*, 509–517.
Serikawa, Y., Shirakawa, M., Matsuo, H., & Kyogoku, Y. (1990) *Protein Eng. 3*, 267–272.
Serikawa, Y., Shirakawa, M., & Kyogoku, Y. (1992) *FEBS Lett. 299*, 205–208.
Shaka, A. J., Barker, P. B., & Freeman, R. (1985) *J. Magn. Reson. 64*, 547–552.
Shaka, A. J., Lee, C. J., & Pines, A. (1988) *J. Magn. Reson. 77*, 274–293.
Spera, S., & Bax, A. (1991) *J. Am. Chem. Soc. 113*, 5490–5492.
States, D. J., Haberkorn, & Rubren, D. J. (1982) *J. Magn. Reson. 48*, 286–292.
Stockman, B. J., Nirmala, N. R., Wagner, G., Delcamp, T. J., DeYarman, M. T., & Freisheim, J. H. (1992) *Biochemistry 31*, 218–229.
van Nuland, N. A. J., van Dijk, A. A., Dijkstra, K., van Hoesel, F. H. J., Scheek, R. M., & Robillard, G. T. (1992) *Eur. J. Biochem. 203*, 483–491.
Wang, J., Mooberry, E. S., Walkenhorst, W. F., & Markley, J. L. (1992) *Biochemistry 31*, 911–920.
Wishart, D. S., Sykes, B. D., & Richards, F. M. (1991) *J. Mol. Biol. 222*, 311–333.
Wüthrich, K. (1986) *NMR of Proteins and Nucleic Acids*, Wiley Interscience, New York.
Wüthrich, K., Billeter, M., & Braun, W. (1983) *J. Mol. Biol. 169*, 949–961.